

Comprehensive Full-Depth Evaluation of Concrete Bridge Decks Based on GPR Surveys and Machine Learning

Arezoo IMANI¹, Shahin SAADATI¹, Nenad GUCUNSKI¹

¹ Rutgers University, Piscataway, USA

Contact e-mail: gucunski@soe.rutgers.edu

ABSTRACT: The traditional practice for condition evaluation of concrete bridge decks using GPR is limited to the condition of the deck above the top reinforcement mat without providing any useful information about the state of concrete below. In an attempt to expand the GPR evaluation zone beyond the top rebar, this study examines a machine learning algorithm as an alternative to the traditional GPR data analysis. Gradient boosting was used to analyze a dataset compiled through GPR surveys of four concrete bridge decks in the United States and to construct a learning algorithm for the purpose of analyzing other experimental GPR data. Two independent prediction modules were developed: *Module 1* to predict the condition above the top rebars, and *Module 2* to predict the condition of concrete in between the top and bottom rebars. A validation test slab in the laboratory was surveyed using the same GPR system, and the data were used to validate the algorithm. The implementation of the proposed method in the validation phase showed that using machine learning and a vast library of GPR data, it is possible to avoid the subjective 90th percentile depth correction for new bridges without compromising the ability to assess the deck condition accurately.

1 INTRODUCTION

A 2011 research by the Rand Corporation found that investment in highway infrastructure can boost the economy through improving productivity and output. The same report showed that in addition to quantity, the quality and condition of the highway system is a significant factor in improving economic activities [1]. Considering the significance of bridges in the greater highway system, the proper management, preservation maintenance, and rehabilitation of bridges are critically important. Inspection and health monitoring are essential elements of bridge management needed for appropriate planning and scoping of maintenance and rehabilitation activities. This is particularly true for bridge decks, which deteriorate faster than other bridge elements, and which inspection and rehabilitation disrupt mobility. GPR allows for large swathes of the deck to be scanned in a short period and with high accuracy and provide an objective assessment of the deck condition. Despite all the advantages of GPR over the traditional methods of bridge deck condition assessment and detection of localized damages in the top section of the deck above the top reinforcing bars and does not provide any information about the condition of the deck below. This study examines a machine learning approach to extend the GPR evaluation zone passed the top section.

The use of machine learning in analyzing GPR data, particularly the use of neural networks and pattern recognition for automatic selection of hyperbolas and rebar detection, has been gaining momentum in recent years [2, 3, 4, 5]. Travassos et al. compiled a review of some of the notable publications in which the use of machine learning or neural networks were used in post-

processing GPR data [6]. A learning algorithm based on gradient boosting was developed using a dataset of experimental data generated via GPR surveys of four bridge decks. The algorithm was used to evaluate the condition of the deck above the top rebar, as well as the condition of the portion of the deck encompassing the top and bottom bars. The algorithm was validated using a validation slab. In the following section, the data collection procedure, as well as the initial data preparation for machine learning, explained. After establishing the targets or the condition indices, a learning algorithm is constructed and applied to independent experimental data.

2 DATA COLLECTION

The GPR data used in this study were collected as part of the U.S. Federal Highway Administration's (FHWA's) Long-Term Bridge Performance (LTBP) Program. The GPR surveys were primarily conducted using a GSSI 1.5 GHz antenna and a SIR-20 control unit. The data were collected using different gain settings for each bridge. The survey lines were 2-ft apart, with the first line being 1-ft away from the curb and parallel to the traffic as the top reinforcing bars were in the transverse direction. Four bridges representing different conditions were selected to develop the experimental dataset for this study: After time-zero adjustment and background removal, the reflection amplitudes and corresponding two-way travel times for the top and bottom rebars were extracted by picking the hyperbolas directly from the B-scans in the 3D profile of each bridge in RADAN 7 [7]. The amplitudes were extracted in data units and later converted into NdB. Instead of using the maximum measurable amplitude by the control unit (2^{15} for SIR-20) for normalizing the amplitudes, the average direct-coupling reflection was used as suggested by Dinh et al. [5]. Using an average direct-coupling reflection helps eliminate the effect of different power or gain settings at the time of data collection. The direct-coupling reflections may vary throughout the deck depending on the surface condition, for example, due to the presence of patches or pothole. However, those remain relatively stable for a given bridge, regardless of concrete conditions.

3 CONDITION INDICES

In the numerical simulations performed previously [8], discrete values called condition indices were assigned based on known electromagnetic properties of simulated concrete and were used later as targets of machine learning. Given the limited amount of ground truth information for the experimental data, the condition indices had to be assigned through a modified depth-correction approach.

To establish these targets for the experimental data, and to demonstrate that the condition indices are an appropriate replacement for the amplitude and TWTT, the contour maps were plotted based on both attenuation and condition indices. It was demonstrated that the two contour maps were very much alike, indicating that it is acceptable to use the condition indices for machine learning purposes, instead of the amplitudes. After it was established that the two contour maps were quite comparable, the condition indices could be used as the ML targets. Since the bottom rebar attributes are not useful features in predicting the condition of the top layer, two different modules (or sub-algorithms) were constructed to predict: (i) R_t (the top concrete layer index), and (ii) R_b (the middle layer concrete layer index).

3.1 Top Layer

Reflection amplitudes for each bridge were first analyzed using the traditional 90th percentile depth correction method. Figure 1 depicts the 3D representation of the reflection amplitudes for

the top reinforcing bars for Pequea Bridge. A combined total of 30,696 data points were extracted for the top reinforcing bars for all four bridges. The reflection amplitudes for both the top and bottom bars for all four bridges are presented in Figure 2. The reflection amplitudes corresponding to sound areas of all bridges were extracted, and the best fit linear regression line was calculated. The coefficient of determination, r^2 , for this linear regression was 0.86. The regression line serves as a reference to identify the concrete condition. For a given two-way travel time, this line returns the amplitude for a hypothetical bar in an area of the deck with a good condition at the top layer. The top rebar amplitudes and the reference line for the sound deck are shown in Figure 2 (a).

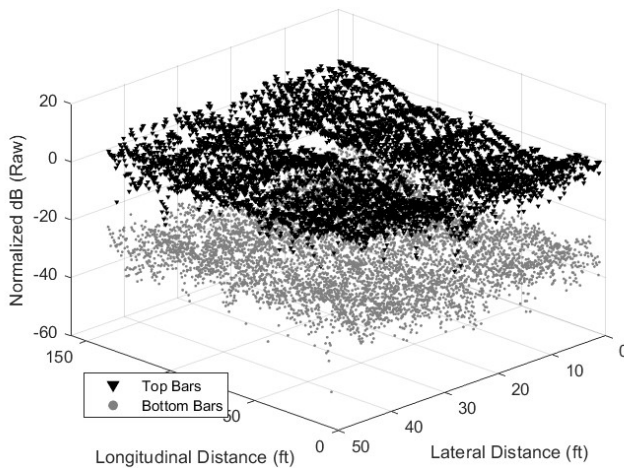


Figure 1. Spatial representation of normalized top and bottom rebar reflection amplitudes (Pequea Bridge).

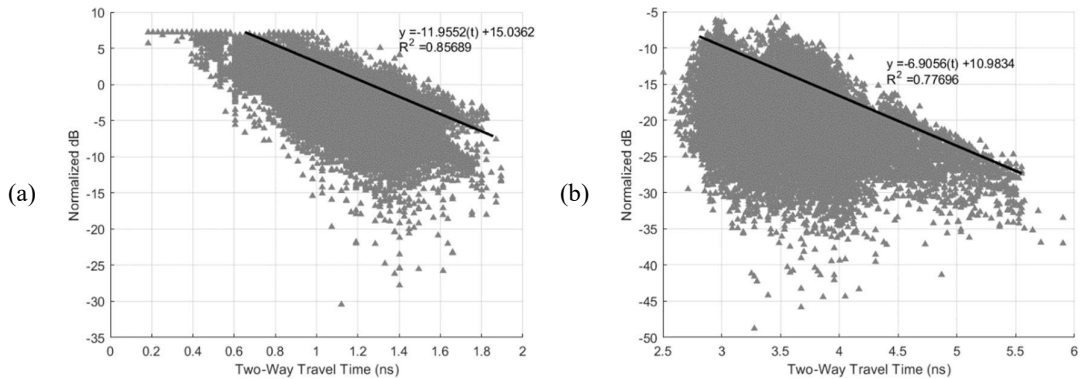


Figure 2. Raw top reflection amplitudes for all bridges: (a) top rebars, (b) bottom rebars.

Following the new depth correction approach introduced by Dinh et al. (2016), individual amplitudes for each bridge were subtracted from the reference amplitude. For a given two-way travel time, the survey amplitudes greater than the reference amplitude based on the linear regression were considered sound. Conversely, survey amplitudes less than the reference amplitude for a given two-way travel time were deemed to be associated with reinforcement in a deteriorated concrete. This approach was modified to generate a condition index for each measured amplitude. The subtracted amplitudes for each bridge were assigned a rating number 0, 30, 60, and 100 representing the top layer of the deck in sound, fair, poor, and serious conditions, respectively (Table 1). In the last column of the table, y represents the experimental amplitude, and \hat{y} is the reference amplitude based on the linear regressions. A representative

attenuation map is compared with the condition maps based on the condition indices for in Figure 3.

Table 1. Concrete condition rating (top layer)

Condition of the Deck	Condition Index	$y - \hat{y}$
Sound	100	> 0
Fair	60	$-5 < < 0$
Poor	30	$-7 < < -5$
Serious	0	< -7

3.2 Middle Layer

The same procedure was used to assign the condition indices for the second layer of the deck encompassing both the top and bottom rebar mats. The only difference was that in the traditional depth correction for the second layer, it was assumed that 20% of each deck was in sound condition as opposed to the typical 10% for the top section. Figure 2 (b) illustrates the collection of the bottom attenuation as well as the reference amplitude line.

During the rebar picking in RADAN 7, a total of over 30,000 hyperbolas were picked, while approximately 26,000 hyperbolas were picked for the bottom bars. This does not affect the algorithm for evaluating the top section as the attributes for the bottom rebar have no bearing on the condition of the deck above top rebar. However, it means that the number of input features is not the same for the second layer. Additionally, it was shown through numerical simulations that the ratio of the attenuation at the top rebar to the attenuation at the bottom rebar is an essential feature in the evaluation of the middle layer [8].

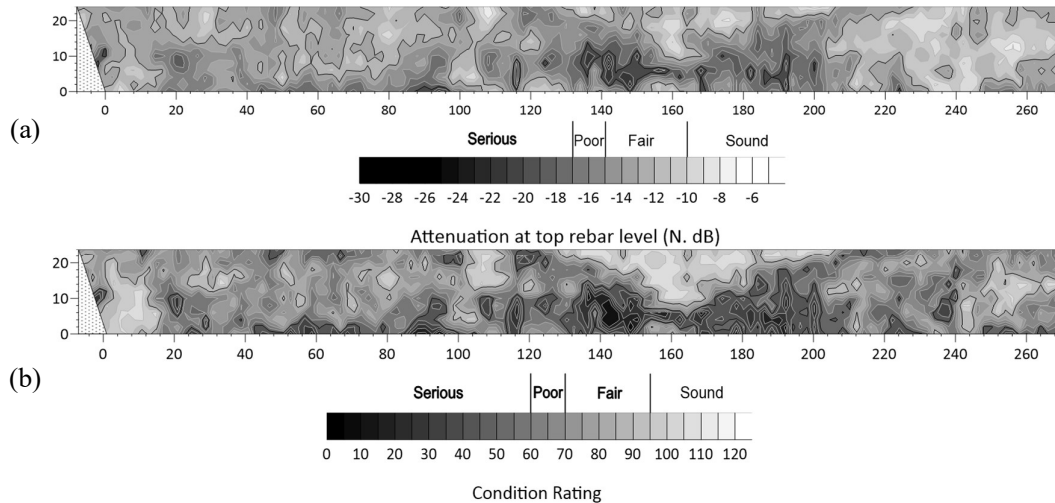


Figure 3. Condition maps for the top layer of Deptford Bridge: (a) GPR based on traditional depth correction, (b) GPR based on new depth correction and condition index.

To resolve these two issues, a data reduction procedure was employed in which at every foot of a given survey line, the minimum raw amplitude was selected discarding the other hyperbolas over that foot. This method of data reduction provides a more conservative condition assessment of the deck below the top reinforcing bars. Figure 4 (a) depicts all the raw amplitudes for the top and bottom rebars associated with the survey line L on Deptford Bridge. Figure 4 (b)

demonstrates the same survey line after data reduction. The data-reduced image is sparser, but the two plots are not significantly different.

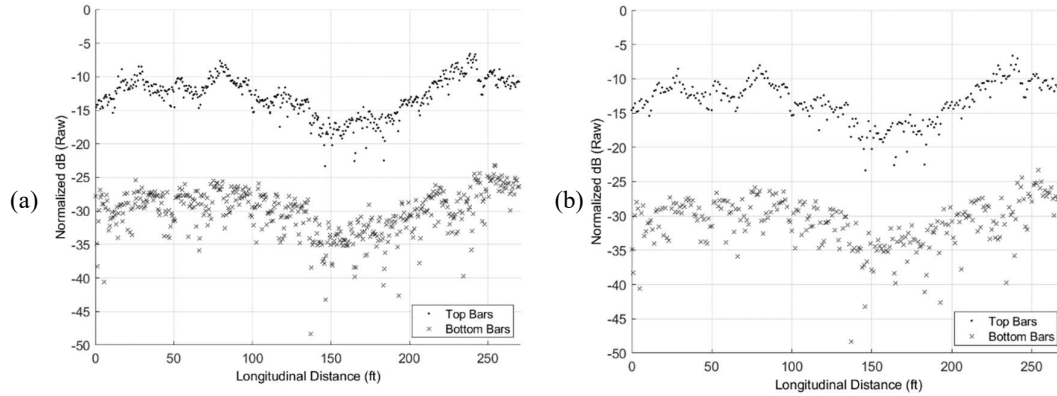


Figure 4. Survey Line L, Deptford Bridge; (a) all the raw amplitudes, (b) minimum amplitudes over every one foot of the survey line.

One indication of deterioration below the top reinforcing bars is that there is a significant attenuation at the bottom rebar compared to the top rebar at the same location. Therefore, for each bridge and after data reduction, the attenuation difference between the top and bottom bars were calculated. Additionally, the average of attenuation drops and the standard deviations were calculated. If the attenuation drop at a given location was more than the overall average plus hundred and twenty percent of the standard deviation, the middle layer was assumed to be in a serious condition. In other words, an additional criterion for the serious condition was defined as follows:

$$Amp_{Bottom} - Amp_{Top} > \mu + 1.2 \times \sigma \quad (1)$$

Where Amp_{Bottom} is the attenuation at the bottom rebar, Amp_{Top} is the attenuation at the top rebar, μ is the global average for a given bridge, and σ is the standard deviation.

The rationale behind this criterion is that the state of the middle layer depends on the attenuation between the top and bottom rebars. Therefore, a significant attenuation at the bottom rebar level compared to the top rebar could be indicative of concrete in a poor condition.

4 LEARNING ALGORITHM

4.1 Module 1 (Top Layer Assessment)

The learning algorithm for module 1 uses three input features: reflection amplitude from the top rebars, the two-way travel time for the top rebar, and an artificial feature which was the exponential function of the amplitude, or $\exp(Amp_T)$. The target values were the condition indices.

$$X^{(i)} = \{AmpT, Tt, \exp(AmpT)\}$$

$$Y^{(i)} = \{Rt\} ; Rt = \{0, 30, 60, 100\} \quad (2)$$

The goal was developing a model for predicting the condition indices for other bridges and the laboratory slab without the need to do individual depth corrections.

A total number of 30,696 $\{(X^{(i)}, Y^{(i)})\}$ data points were used for this algorithm. The data set was randomly split into two sets: (a) 70% to train the algorithm and fine-tune the parameters, and (b) 30% to validate the learned model. The training set and the test set were independent of one another. The best accuracy for the test set was over 98% for the assumptions that were made in

the definition of condition indices. The main assumption was that the condition indices for the four bridges used for constructing the model were correct and providing ground truth. The feature importance was also evaluated. The two-way travel time has the highest impact followed by the amplitude. The feature importance is summarized

Table 2. Feature Importance (Module 1)

Feature	Importance (%)
Tt	49.77
AmpT	25.90
exp(AmpT)	24.33

To validate the learning algorithm, the GPR data for a validation slab was processed. The condition indices were calculated based on the modified depth correction approach. The raw amplitudes and the TWTT's were fed to the model based on the original four bridges. Out of 495 points, the algorithm predicted the condition index of 491 points correctly. This indicated the potential for avoiding the use of arbitrary depth correction for a new bridge as long as a learning algorithm can be developed based on several bridges within a network when the same GPR system is used for data collection. Figure 5 depicts the top rebar amplitudes from the slab superimposed on the top rebar amplitudes for the four bridges. The amplitudes corresponding to sound concrete are shown in pink. The linear regression line is also shown.

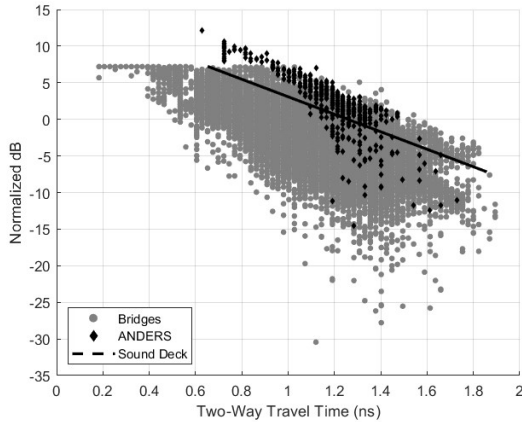


Figure 5. Top rebar reflection amplitudes normalized with respect to the average direct-coupling amplitude. The validation slab amplitudes are shown using black dots.

4.2 Module 2 (Second Layer Assessment)

The learning algorithm for module 2 uses the following input features and targets:

$$\begin{aligned} X^{(i)} &= \{ \text{AmpT}, \text{AmpB}, \text{Tt}, \text{Tb}, \text{exp}(\text{AmpT}), \text{exp}(\text{AmpB}), \text{AmpT}/\text{AmpB} \} \\ Y^{(i)} &= \{ \text{Rt}, \text{Rb} \} ; R_j = \{ 0, 30, 60, 100 \} \end{aligned} \quad (3)$$

The best accuracy for the test set was 79.7%. The feature importance was also evaluated. The reflection amplitude from the bottom rebar has the highest impact followed by the two-way travel time for the bottom rebar (Table 3). The condition maps generated based on the traditional 80th percentile and the new condition index approach are presented in Figure 7. The accuracy of the model in the middle layer condition prediction was 72.7%. This could potentially be improved should a bigger initial dataset be used to construct the model.

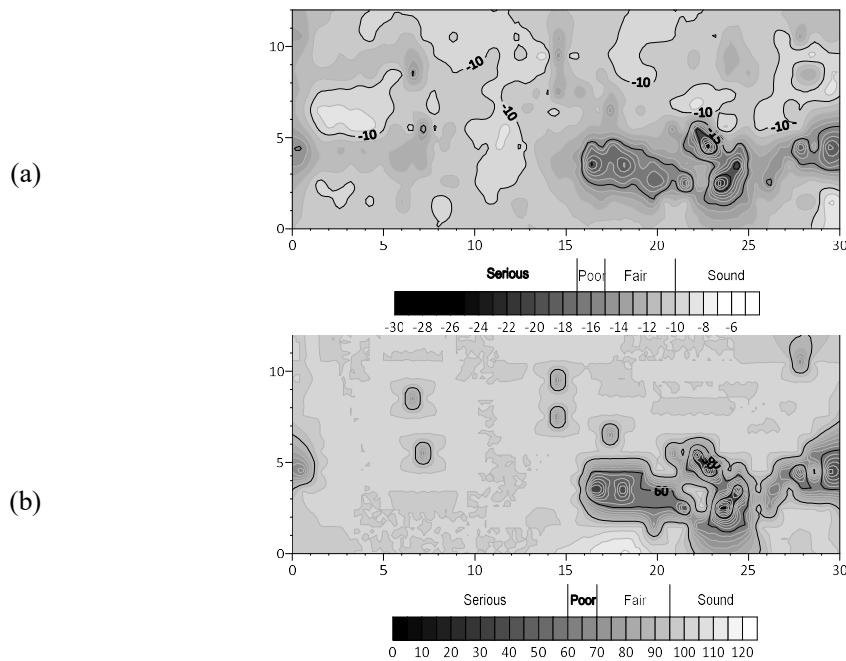


Figure 6. Condition maps for the top layer of the validation slab: (a) GPR based on traditional depth correction, (b) GPR based on new depth correction and condition index.

Table 3. Feature Importance (Module 2)

Feature	Importance (%)
AmpB	50.17
Tb	37.25
Tt	6.16

5 CONCLUSIONS

The primary goal of the present study was to develop a novel data processing technique to expand the GPR evaluation zone beyond the top reinforcement level, thereby providing the full-depth assessment of the deck. Based on a machine learning-based analysis of experimental GPR data and the laboratory implementation, the following main conclusions were made:

- Results of a learning algorithm based on gradient boosting suggest that machine learning is a robust method for expanding the GPR evaluation zone beyond the top reinforcing steel bars.
- The algorithms were limited to evaluating the condition of bridge decks at the top layer, above the top rebar, and the middle layer of the deck, encompassing the zone between the top and bottom rebars as the reflections from the bottom of the deck are not always readily available.
- Provided that a pool of data is generated by putting together the survey results from a more significant number of bridges, an algorithm can be trained for condition evaluation of bridge decks, without the need for the subjective 90th percentile depth correction for every new bridge.

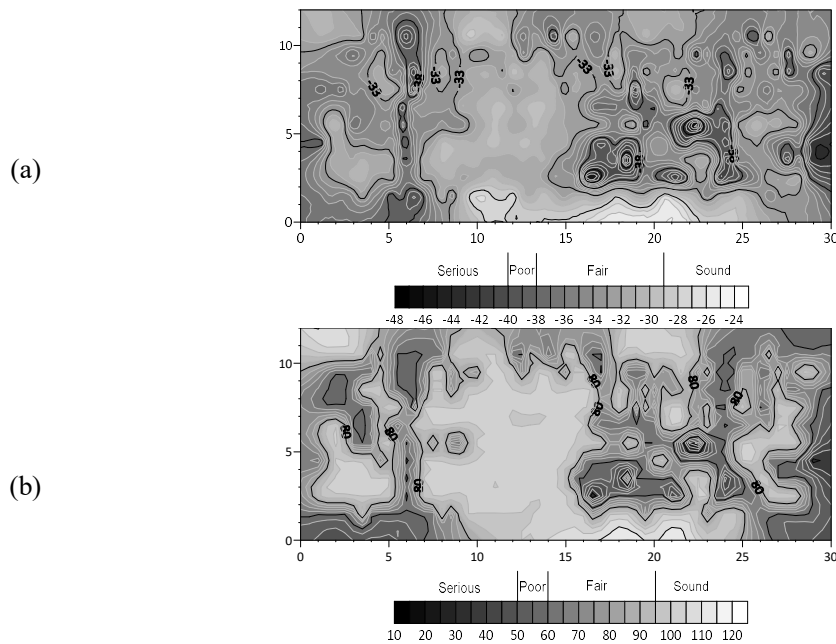


Figure 7. Condition maps for the second layer of the validation slab: (a) GPR based on traditional depth correction, (b) GPR based on new depth correction and condition index.

6 REFERENCES

- [1] H. J. Shatz, K. E. Kitchens, S. Rosenbloom and M. Wachs, "Highway Infrastructure and the Economy: Implications for Federal Policy," RAND Corporation, Santa Monica, CA, 2011.
- [2] N. P. Singh and M. J. Nene, "Buried Object Detection and Analysis of GPR Images: Using Neural Network and Curve Fitting," in International Conference on Microelectronics, Communication and Renewable Energy (ICMiCR-2013), Kerala, India, 2013.
- [3] M. R. Shaw, M. S. G, T. C. K. Molyneaux and M. J. Taylor, "Location of Steel Reinforcement in Concrete Using Ground Penetrating Radar and Neural Networks," NDT & E International, vol. 38, no. 3, pp. 203-212, 2004.
- [4] W. Al-Nuaimy, Y. Huang, M. Nakhkash, M. T. C. Fang, V. T. C. Nguyen and A. Eriksen, "Automatic detection of buried utilities and solid objects with GPR using neural networks and pattern recognition," Journal of Applied Geophysics, vol. 43, pp. 157-165, 2000.
- [5] K. Dinh, N. Gucunski, J. Kim and T. H. Duong, "Understanding Depth-Amplitude Effects in Assessment of GPR Data from Concrete Bridge Deck Surveys," NDT & E International, vol. 83, pp. 48-58, 2016.
- [6] X. L. Travassos, S. L. Avila and N. Ida, "Artificial Neural Networks and Machine Learning techniques applied to Ground Penetrating Radar: A review," Applied Computing and Informatics, 2018.
- [7] "RADAN 7 Manual," Geophysical Survey Systems Inc, Nashua, New Hampshire, 2017.
- [8] A. Imani, S. Saadati and N. Gucunski, "Full-Depth Assessment of Concrete Bridge Decks in A GPR Survey: A Machine Learning Approach," in ASNT SMT-CE, New Brunswick, 2018.